Journal of Hydrology 598 (2021) 126157

Contents lists available at ScienceDirect

Journal of Hydrology

journal homepage: www.elsevier.com/locate/jhydrol

Research papers

A new transfer function model for the estimation of non-point-source solute travel times

Marialaura Bancheri [a,*], Antonio Coppola [b], Angelo Basile [a]

[a] Institute for Mediterranean Agricultural and Forestry Systems (ISAFOM), National Research Council (CNR), Portici (NA), Italy
[b] School of Agricultural, Forestry, Food and Environmental Sciences (SAFE), Hydraulics Division, University of Basilicata, Potenza, Italy

ARTICLE INFO

This manuscript was handled by Jiri Simunek, Editor-in-Chief, with the assistance of Giuseppe Brunetti, Associate Editor

Keywords:
Extended transfer function
Travel times
Hydraulic conductivity curve
Spatial leaching model
Groundwater vulnerability assessment

ABSTRACT

The scope of this work is to present a new fast and reliable transfer function model, which simulates the spatio-temporal distribution of non-point-source solutes along the unsaturated zone, suitable to be used at large scales within a web-based Decision Support System. With the assumptions of a) a gravity induced water flow, b) a non-reactive solute and c) a purely convective flow, the model uses the transfer functions, i.e., the travel time (TT) probability density functions, derived from the unsaturated hydraulic conductivity curve $k(\theta)$. The output concentration of a solute is simply the convolution of the transfer functions with the input concentrations to the system. A model sensitivity analysis, based on Monte Carlo simulations, was carried out, showing that saturated water content and the tortuosity parameter τ were the parameters that affected the mean TT more. The model was validated against concentration experiments carried out on four large soil columns. Results were really good for all soils, with the best agreement with $R^2 = 0.97$, RMSE = 0.11 and ME = −0.01. Moreover, the outputs obtained applying the model to 46 soil profiles sampled in the Valle Telesina, in Southern Italy, completely characterised from the hydrological point of view, were compared with those obtained from the Richard-based model Hydrus 1D. The result of the comparisons gave a very high correlation coefficient (above 0.8), a mean absolute error between the two models of around 40 days and a percent bias of −16%. Finally, the application of transfer function model to a large spatial extent is presented, to show its possible use for the groundwater vulnerability assessment.

1. Introduction

The effort to combine productivity with more sustainable water and soil resources management is imperative in many policies, such as in the United Nations Sustainable Development Goals (https://sustainabledevelopment.un.org) and in the new European Green Deal strategy (https://ec.europa.eu/info/strategy/priorities-2019-2024/european-green-deal_en). More specifically the European Nitrate Directive (Dir. 91/676/EEC), the Pesticide Directive (Dir. 2009/128/EC) and the Water Framework Directive (Dir. 2000/60/EC) state the prioritizing actions to be applied from each EU Member State for the protection and the avoidance of deterioration of waters. However, these policy-maker requests do not always correspond to the availability of really operational tools.

The study of Non-Point Source (NPS) chemical contaminants requires a multidisciplinary approach, which encompasses hydrology, soil science, as well as spatial statistics and geographic information systems (Coppola et al., 2013a), since they are widespread at local, regional, and global scales.

Several spatial leaching modelling systems were proposed in recent years. In Petach et al. (1991), LEACH-M was used to simulate the movement of four classes of chemicals through layered soils, for pesticide management and for estimating potential leaching hazards; Zhang et al. (1996) combined an index and overlay model, i.e., the DRASTIC model (Aller, 1985), with the process-based numerical model HYDRUS (Simunek et al., 1998, 2012). Vero et al. (2017) also proposed an HYDRUS-based framework, which considered existing soil maps, meteorological data and different land use, to estimate solute time lags at catchment scale. The Root Zone Water Quality Model (RZWQM) (Ahuja et al., 2000; Kumar et al., 1999) is a process-based agricultural model that can be applied to quantify the effect of nitrate leaching through the vadose zone on the environment. PEARL/GeoPEARL (Tiktak

* Corresponding author at: Institute for Mediterranean Agricultural and Forestry Systems (ISAFOM), National Research Council(CNR), Piazzale Enrico Fermi, 1, Portici (NA), Italy.
E-mail address: marialaura.bancheri@isafom.cnr.it (M. Bancheri).

https://doi.org/10.1016/j.jhydrol.2021.126157
Received 10 November 2020; Received in revised form 2 February 2021; Accepted 1 March 2021
Available online 9 April 2021

et al., 2002) was used to calculate the leaching potential of pesticides into local surface waters and the regional groundwater considering the soil type, land use, climate and groundwater depth class for 6405 plots, combining the 1D pesticide leaching model, PEARL, with a Geographical Information System. Holman et al. (2004) proposed the MACRO emulator, a spatially distributed modelling system for predicting pesticide losses to groundwater. Eventually, the user-friendly, GIS-based and client-server software VULPES, based on PELMO leaching model (Di Guardo and Finizio, 2015), was developed to identify vulnerable areas at regional level.

However, despite their wide use, these models fail to be really operational for policy applications, being mostly based on desktop solutions, often too computational demanding. Moreover, these approaches often fail in the crucial interaction between end-users and scientists, well defined by the following statement, taken by Bouma et al. (2008): "*Rather than following traditional top-down and disciplinary research approaches, emphasis is increasingly being placed on interactive, interdisciplinary work in Communities of Practice (CoPs) in which scientists work together with various stakeholders and policymakers in a joint learning mode*".

In order to fulfill these requests, in the last decade, much progress has been accomplished in development of geo-spatial decision support systems — freely available on the web – explicitly accounting for water flow and transport of dissolved contaminants through the vadose zone at different spatio-temporal scales (Terribile et al., 2015). These systems allow the so-called on-the-fly modelling, in support of the what-if scenario procedures. In this context, the use of high CPU-demanding models, based on numerical solutions is not advisable (e.g., Richards combined with Advective-Dispersion equation). Therefore, the aim of this work is to present the extended Transfer Function model (TFM-ext) for the estimation of the travel times of the NPS, which promises to be a fast and reliable tool for the groundwater vulnerability assessment in support of the previously cited Directives, within the larger Spatial-Decision Support System (S-DSS) developed for LandSupport H2020 project (https://www.landsupport.eu).

The work is organized as follows: Section 2 presents the rationale behind the need of the TFM-ext model. Section 3 presents i) the theory behind the model, ii) the sensitivity analysis to its parameter variations trough a Monte Carlo technique, iii) its validation using four large undisturbed soil columns, iv) the comparison with the physically-based model Hydrus 1D and v) the application at the Valle Telesina extent in support of the groundwater vulnerability assessment. Section 4 describes the Valle Telesina and the hydraulic properties dataset. Section 5 reports and discusses the results of the TFM-ext testings and comparisons. The conclusions of the study are given in Section 6.

2. Rationale behind the development of TFM-ext

In order to let the interested reader enter in the rationale behind the TFM-ext model within a web-based S-DSS, we try to do a simple example of a typical problem we would face: a regional policy maker should define the zones vulnerable to nitrates and pesticides in a selected Region of Interest (ROI). In this ROI, let's suppose of around 50 km^2, we distinguish: 4 soil polygons, with different hydraulic characteristics, 6 different land uses (different crops), 2 climates (a part of the ROI is uphill) and a groundwater table depth, variable for each point of the domain.

Besides the spatial variability, the policy maker wants also to consider the time evolution of nitrate and pesticide leaching, both with past and future scenarios. Let's consider that, again for simplicity, the policy maker is only interested in 2 particular years of simulation.

Combining the spatial and temporal variability of the variable considered, to give an answer to the policy maker, we need to run, at most, around 400 simulations (if we make a further simplification on the groundwater table depth). The policy maker, though, wants a real-time answer to his/her problem, which should also be effective, clearly understandable, on a dynamic map, freely accessible on the web. And he/she also wants to be able to consider another ROI (with different crops), bigger than the previous one, and a longer simulation, of 10 years for example. In such a case the number of required simulations will increase by orders of magnitude. It is important to stress that, most of times, the end-users are not modellists, used to play with partial differential equations and possible related problems (multiple parameters definition, possibility of not convergence of the solutions, climatic issues and so on). This situation should be absolutely avoided, in order to have the widest application of the models in the community, overcoming the historical trade-off between the research-scientific world and the everyday real-life applications requiring effective, clear and real-time answers (Bouma et al., 2008; Bouma, 2015).

Is there a model able to help the policy maker considering all the previous needs, in a fast and a physically meaning ways, giving him/her an immediately interpretable answer to his/her problems? The last is our key science question, which we are trying to answer by proposing the TFM-ext model, to be implemented within a web-based Spatial-Decision Support System (S-DSS). The use of these systems, in fact, through dedicated full open-access platform, allows real-time responses and the production of scenario analysis by different end-users queries. They are not simply Web-GIS system, but dynamic environments that could address many different issues, from forest resources management (Marano et al., 2019) to olive growing (Manna et al., 2020) and more.

3. Methods

TFM-ext is based on Jury's transfer functions (Jury, 1982; Jury and Roth, 1990), which are defined as the probability density functions of the travel times at a given time and depth. Transfer functions are widely used in several disciplines such as in catchment hydrology (Botter et al., 2011; Rinaldo et al., 2011; Rigon et al., 2016b), in population dynamics and demography (Bongaarts and Feeney, 2003) and more (Calabrese and Porporato, 2015; Rigon et al., 2016a). They allow to compute the output concentration of a solute by simply convolve the transfer functions with the input concentrations to the system.

In this work the transfer functions are derived from the hydraulic conductivity functions, defined for each layer of the unsaturated zone, starting from the approach reported in Scotter and Ross (1994).

Other simplified models, based, for example, on the estimation of the unsaturated vertical subsurface travel time (e.g., Lee and Casey, 2005; Fenton et al., 2011; Sousa et al., 2013; Szymkiewicz et al., 2018, 2019) despite being very effective, don't compute the output solute flux concentration, in time and depth, as we can do using the transfer functions.

It is important to stress that TFM-ext is not intended to describe in details local scale transport behaviour, but, as already reported in Section 3,it was thought to fulfil the following objectives:

- to integrate a simplified statistical approach with physically-based hydrological parameters;
- to be valid for large scale applications but still keeping a physical meaning;
- to be easy to interpret.

3.1. Model description

According to the Jury's transfer function model, TFM-ext computes the output solute flux concentration $C_z(z,t)$ [ML^{-3}], at a given depth z and a given time t as follows:

$$C_z(z,t) = \int_0^T C_o(0,t')f_f(z,t-t')dt' \quad (1)$$

where $C_0(t)$ [ML^{-3}] is the solute concentration at the surface, t$'$ is a dummy variable and $f_f(z,t)$ is the Travel Times probability density

function (TT-pdf), for a travel distance z, conditional to time t. In this study, a time-invariant form of the TT-pdf was assumed, since the solution of the water budget within the specific control volume is a key point to apply the time-variant theory (e.g., Botter et al., 2011; Rinaldo et al., 2011; Harman, 2015; Rigon et al., 2016b). If, for simplicity, we consider a simple bucket model, with a linear reservoir, one for each soil layer, we have as a minimum 2 parameters to be defined, i.e., to be calibrated. After the previous discussion made in Section 2, on the spatio-temporal variability of our policy maker request, adding parameters to be calibrated and ordinary differential equations to be solved would not be an easy task for our problem. The situation is even worse if we consider solving Richards equation, which would be actually required to have the correct solutions of the water budget at this scale of interest.

According to Scotter and Ross (1994), TFM-ext derives the TT pdfs from the unsaturated hydraulic conductivity $k(\theta)$, with the assumptions of a) a gravity-induced water flow, b) a conservative and nonreactive solute and c) a purely convective flow, as follows:

$$f_f(z,t) = -\frac{1}{q}\frac{dk(\theta)}{dt} \tag{2}$$

where $f_f(z,t)$ [T^{-1}] is the travel time pdf, q [LT^{-1}] is the steady state flow rate, $k(\theta)$ [LT^{-1}] is the hydraulic conductivity function, and θ [–] is the water content.

The steady state flow rate q can easily be derived from a water budget at the control volume, considering constant input fluxes (e.g., constant mean daily net precipitation) at the surface boundary.

For a given steady-state flow rate q, Eq. (2) allows to derive the TT-pdf for each horizon of soil profile, starting from the corresponding $k(\theta)$curve.

The hydraulic conductivity function was assumed to be described by the van Genucthen-Mualem (VGM) equations (Van Genuchten, 1980):

$$k(\theta) = k_0 S_e^{\tau}[1-(1-S_e^{1/m})^m]^2 \tag{3}$$

$$S_e = \frac{\theta-\theta_r}{\theta_s-\theta_r} = [1+|\alpha h|^n]^{-m} \tag{4}$$

where S_e is effective saturation, h [L] is the pressure head, α [L^{-1}] is related to the inverse of the air entry pressure head, n [-] and m [-] are shape parameters, with the constrain that $m = 1-1/n, \theta, \theta_r$ [–] and θ_s [–] are the actual, the residual and the saturated water contents, respectively, k_0 [LT^{-1}] is the hydraulic conductivity at $\theta = \theta_s$ and τ is a parameter which accounts for the dependence of the tortuosity and the correlation factors on the water content. The time derivative of the hydraulic conductivity function, according to Eq. (2), is reported in Appendix A. $k(\theta)$ can be made varying with time, which is actually the travel time and not the clock time, with some simple variable substitutions. We could also reverse the concept, i.e., we can look at the travel time variation related to the variation of water content and, thus, of the hydraulic conductivity.

Some considerations about the hydraulic conductivity function help to better understand the involved transport processes. In particular, in Fig. 1, θ' is the actual water content induced in the soil by q. Thus, assuming a unit gradient, $q = k(\theta)$ and $dq/d\theta'$ identifies the largest pore pathway where the maximum velocity is reached. The pores corresponding to $\theta > \theta'$ are not involved in the water flow and thus are not accounted in Eq. (2).

Once the TT-pdf is derived for each horizon, the solute transport along the whole soil profile requires an additional hypothesis on the correlation among travel times in the different horizons (Hamlen and Kachanoski, 1992). We assume that the travel times of a solute particle in one soil horizon are uncorrelated to the travel times to the other soil horizons. In this case, the entire soil profile can be described by the first and second moments, i.e., the mean and the variance of the

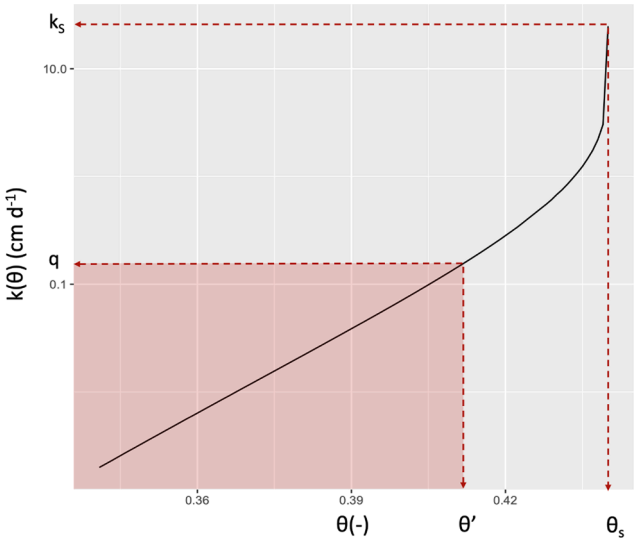

Fig. 1. Unsaturated conductivity curve $k(\theta)$: the red shaded area represents the part of the curve involved in the transport processes according to the proposed model. (For interpretation of the references to color in this figure legend, the reader is referred to the web version of this article.)

breakthrough curve $C_z(z,t)$ (Hamlen and Kachanoski, 1992) and can be computed as follows:

$$E(z,t) = \sum_{i=1}^{m} E_i(z,t) \tag{5}$$

$$Var(z,t) = \sum_{i=1}^{m} Var_i(z,t) \tag{6}$$

where $E(z,t)$ and $Var(z,t)$ are the mean and the variance of the travel times to depth z, m is the number of the soil horizon and $E_i(z,t)$ and $Var_i(z,t)$ are the mean and variance on the $i-th$ horizon, respectively.

In particular, the mean and the variance of the travel times are calculated according to Leij and Dane (1991) as follows:

$$M_i^n(z,t) = \frac{\int_0^\infty t^n[1-C_z(z,t)]dt}{\int_0^\infty [1-C_z(z,t)]dt} \tag{7}$$

where n is the order of the moment (i.e., 1 for the mean $E_i(z,t)$ and 2 for the variance $Var_i(z,t)$) and $C_z(z,t)$ is the concentration of the solute at the time t and depth z.

In the present study, the upper limit of the moment integrals was bounded considering the time t at which 98% of the total input mass injected at the surface was recovered at the investigated depth z. In this way, the possible long tail of the travel time distributions didn't affect the moment computations, avoiding uncertainties in the numerical calculation of the integrals.

Let's assume now that we are interested in transport to depths greater than the soil depth for which the TFM-ext has been developed, e.g., below the soil profile till the groundwater table level. Let's define:

- z: the depth to which we have all the information on the hydraulic parameters;
- l: the depth of interest, where l is greater than z.

Between z and l, the properties governing the transport are unknown.

To extend the process till l, we used the Generalized Transfer Function (GTF) proposed by Zhang (2000), which assumed a lognormal form for the travel times distribution, expressed as follows:

$$f_f(l,t) = \frac{1}{(2\pi)^{0.5}\sigma(l,t)t} exp\left(-\frac{(ln(t) - \mu(l,t))^2}{2\sigma(l,t)^2} \right) \quad (8)$$

where $\mu(l,t)$ and $\sigma(l,t)$ are the moments of the $ln(t)$, at the depth l. They can be obtained by inverting the following relations with the mean and the variance of the travel times at depth l:

$$E(l,t) = exp\left(\mu(l,t) + \frac{\sigma(l,t)^2}{2}\right) \quad (9)$$

$$Var(l,t) = exp(2\mu(l,t) + \sigma(l,t)^2)[exp(\sigma(l,t)^2) - 1] \quad (10)$$

where, according the GTF, $E(l,t)$ and $Var(l,t)$ are assumed to scale with depth, between z and l, as follows:

$$\frac{E(l,t)}{E(z,t)} = \left(\frac{l}{z}\right)^{\lambda_1} \quad (11)$$

$$\frac{Var(l,t)}{Var(z,t)} = \left(\frac{l}{z}\right)^{2\lambda_2} \quad (12)$$

λ_1 and λ_2 are the parameters that account for the propagation of the travel time moments, which allow to classify the transport process according to the difference $\lambda_1 - \lambda_2$: i) if $\lambda_1 - \lambda_2 = 0$, the process is stochastic–convective; ii) if $\lambda_1 - \lambda_2 < 0$, the process is scale-dependent; iii) if $\lambda_1 - \lambda_2 = 0.5$ the model is convective–dispersive (Zhang, 2000). Since we are considering uncorrelated travel times between layers, then $\lambda_1 - \lambda_2 = 0.5$ and the process is convective–dispersive (Jury, 1982; Jury and Roth, 1990).

In summary, for each soil horizon between the surface and z, where we assume to know all the hydraulic parameters, we can calculate the TT-pdf through the Eq. (2). Between z and l, we assume a lognormal form of the TT pdf, according to the GTF, whose parameters are computed from the mean and the variance of the travel times at depth z, Eqs. (9) and (10), which are scaled with the power of the ratio of z and l, according to Eqs. (11) and (12).

3.2. Sensitivity analysis

The sensitivity of the proposed TFM-ext model to the variation of the parameters $\theta_r, \theta_s, \alpha, n, k_0, \tau$ was tested using the dataset of the measured hydraulic properties of the soils of the Valle Telesina site, fully described in Section 4.

Firstly, the correlation matrix was computed and the Cumulative Distribution Function (CDF) was derived for $\theta_r, \theta_s, \alpha, n, k_0, \tau$ (Carsel and Parrish, 1988). Where the normality was directly obtained, the normal Gaussian distribution was adopted; otherwise, a transformation was applied to achieve normality. In particular, three transformed normal distributions, known as the Johnson system (Johnson et al., 1970), were chosen:

1. lognormal (LN): $Y = ln(X)$
2. log ratio (SB): $Y = ln[(X - A)/(B - X)]$
3. hyperbolic arcsine (SU): $Y = sinh^{-1}[U] = ln[U + (1 + U^2)^{1/2}]$

where X is the untransformed parameter, A and B are the upper and lower bounds of the investigated parameter, and $U = (X - A)/(B - A)$. In order to choose the best fitting distribution for each parameter the Kolmogorov–Smirnov test was used.

Then, to test the model sensitivity, a Monte Carlo approach was used to generate N sets of realizations of the investigated parameters. Two cases were considered a) all parameters as correlated and b) all the parameters as not correlated (Smith and Diekkrüger, 1996; Coppola et al., 2009).

In the case of correlated parameters, the random fields were obtained with a Monte Carlo procedure from the correlated multivariate normal distribution, by generating a vector r_n of independent standard normal deviates and then applying a linear transformation of the form $x = \mu + Lr_n$, where μ is the vector of means and L is the lower triangular matrix derived from the symmetric covariance matrix $V = LL^T$, decomposed by Cholesky factorization, according to Carsel and Parrish (1988).

To help the interpretation of the results of the sensitivity analysis, the relative importance index toward the variance (RI_p) of the travel times (Paleologos and Lerche, 1999; Avanidou and Paleologos, 2002) and the relative deviation method (RD) (Hamby, 1995) were computed. In particular, the first was computed as follows:

$$RI_p = \frac{\sigma^2_{T_p}}{\sum_{p=1}^{p}\sigma^2_{T_p}} \quad (13)$$

where p is the $p-th$ parameter we are considering and $\sigma^2_{T_p}$ is the variance of the travel times obtained varying the $p-th$ parameter.

The RD was computed as:

$$RD = \frac{\sigma_{T_p}}{\mu_{T_p}} \quad (14)$$

This index measures the amount of variability in the model output while varying each input parameter, one at a time, according to its probability density function, and it is similar to a coefficient of variation.

Eventually, the model sensitivity toward the variation of the steady state input flux was tested, while keeping the investigated parameters fixed to their mean.

3.3. Soil columns validation

The validation of the model was performed by using data from previously conducted experiments on large undisturbed soil columns (between 70 and 120 cm high, 40 cm in diameter), as detailed reported in Coppola et al. (2004).

The columns, as represented in Fig. 2, were fed by means of a tension infiltrometer hydraulically connected to a Mariotte bottle. The steady-state flow rates used during the experiments were: 130 $cm\ d^{-1}$ for column P1, 100 $cm\ d^{-1}$ for column P3, 200 $cm\ d^{-1}$ for column P4 and 35 $cm\ d^{-1}$ for column P5.

Double wire time domain reflectometry (TDR) probes were inserted at different depths to monitor water content and solute resident concentrations during water infiltration and solute transport experiments.

The parameters of the water retention and hydraulic conductivity functions of the columns, reported in Table 1, were obtained by solving an inverse problem of parameter estimation.

The solute resident concentrations, C_r [–], were derived from transmission line (TDR probe) impedance measurements. For further details on the experimental methodology, the interested reader can refer to Coppola et al. (2004).

The columns – belonging to four different soils – were selected as test cases for the present work, whose texture, organic matter content and hydraulic parameters are reported in Table 1:

3.4. Hydrus 1D comparison

The model Hydrus 1D (Simunek et al., 2016) was chosen for a comparison of the results of the TFM-ext obtained for a large spatial scale application. Hydrus 1D numerically solves the Richards equation for variably-saturated water flow and advection–dispersion type equations for solute transport. The flow equation incorporates a sink term to account for water uptake by plant roots (see Table 2).

For for each soil profile of the Valle Telesina, the following vegetation and upper boundary conditions were considered:

As regards Hydrus 1D, we considered 3 years (2002-2004) of variable precipitation and reference evapotranspiration from the historical dataset. The initial conditions were set with a pressure head equal -100

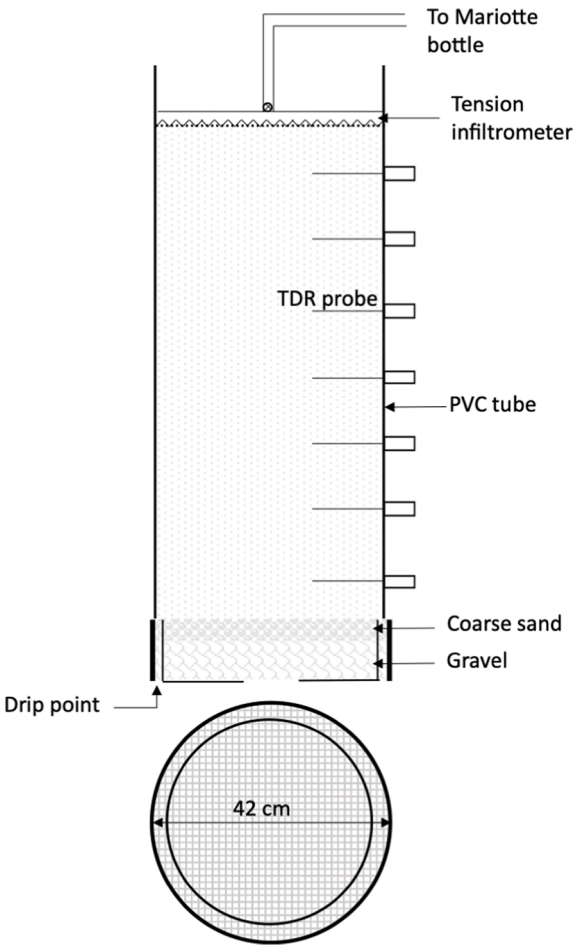

Fig. 2. Schematic representation of the soil column setup. Figure re-drawn from Coppola et al. (2004).

cm, while the lower boundary conditions were set to the free drainage and the zero concentration gradient. The hydraulic conductivity curve was assumed to be described by the VGM model. For the solute transport, the equilibrium model was used and only one non-reactive solute was considered, which was injected the first day of the simulation, with a value of 43.5 mmol l^{-1}. The dispersivity varied between 2.4 and 12.8 cm: for around forty soil samples, it was measured carrying out inflow-outflow experiments with the procedure described in Coppola et al. (2011), while, for the remaining soil horizons, we set the value according to similar textural classes. 150 nodes for each profile (1 cm spacing) were considered. The root water uptake model was chosen the one proposed by Feddes et al., 1978, with no solute stress, where the root parameters were set to literature values of pasture. Accordingly, Leaf Area Index (LAI) and light extinction coefficient were set for the entire period equal to 2 m^2 m^{-2} and 0.39, respectively.

As regards TFM-ext, to obtain the constant flux q, (Eq. (2)):

1. we considered 3 years (2002–2004) of variable precipitation and reference evapotranspiration from the historical dataset;
2. we simulated, using the FAO model (Allen et al., 1998), the actual evapotranspiration, considering the crop and water stress coefficients;
3. we cumulated the annual volumes and computed the constant mean daily net precipitation.

Despite there were really small difference in the cumulated annual volumes of actual evapotranspiration computed by the two models (less than 30 mm $year^{-1}$), they were considered negligible since they didn't affect significantly the mean daily net precipitation.

On the breakthrough curves obtained at the soil profile depth, i.e., 150 cm, the mean and the variance of the travel times were calculated according to Eq. (7) and compared to those obtained with the TFM-ext.

3.5. TFM-ext application at a large spatial extent

As stated in the Introduction and in Section 2, TFM-ext was conceived to be implemented in the S-DSS to predict, in real-time, NPS travel times. Therefore, we present a particular application to the Valle Telesina case study, supposing to be interested to evaluate the filtering capacity of the soils at a fixed groundwater depth of 3 meters. The scope is to better highlight the potentiality of the model for the policy-makers, in support of the definition of the vulnerable areas.

The inputs for the spatial application are for the user-defined area: i) the depth of interest, ii) the soil types, iii) the climate, iv) the land uses

Table 2
Vegetation and upper boundary conditions (BC) for the TFM-ext and Hydrus 1D model.

TFM-ext		Hydrus 1D	
Vegetation	Upper BC	Vegetation	Upper BC
pasture	variable in space and constant in time	pasture	variable in space and time

Table 1
Main soil characteristics and hydraulic parameters of the four soil columns.

Horizon	*z* cm	*Sand* (%)	*Silt* (%)	*Clay* (%)	*o.m.* (%)	θ_r (–)	θ_s (–)	α (cm^{-1})	n (–)	k_0 ($cm\ d^{-1}$)	τ (–)
ProfileP1											
Ap	0 –40	60.33	18.13	21.53	0.88	0.01	0.385	0.0118	1.55	168.8	0.5
Bk1	40 –100	72.00	12.20	15.80	0.14	0.01	0.310	0.0108	1.40	240.0	0.5
ProfileP3											
Ap	0 –20	67.15	16.55	16.30	0.81	0.00	0.25	0.0250	1.27	169.4	0.5
Bt	20 –70	67.60	16.00	16.40	0.47	0.00	0.25	0.0012	1.27	169.4	0.5
ProfileP4											
Ap	0 –50	68.27	13.87	17.87	0.66	0.00	0.30	0.0340	1.50	345.6	0.5
Bt	50 –120	70.35	13.85	15.80	0.23	0.00	0.22	0.0085	1.64	324.5	0.5
ProfileP5											
Ap	0 –20	36.97	42.70	20.33	1.32	0.00	0.36	0.0100	1.33	39.6	0.5
Bt	20 –70	36.90	27.50	35.60	0.78	0.00	0.36	0.0112	1.23	36.5	0.5

and v) the crop managements.

The full characterization of soil layers to 3 meters depth was not available, but only till 1.5 m, as described in Section 4. The climate was considered spatially variable, the land use considered for the entire valley was the alpha-alpha, fertilized with a non-reactive solute of 0.65 mmol l^{-1}.

4. Study case

4.1. Study site

The Valle Telesina site, located in southern Italy, is a 200 km^2 area with five different landscape systems: limestone mountains, with volcanic ash deposits at the surface; hills, comprised of marl arenaceous flysch; pediment plain, comprised of colluvium material from the slope fan of the limestone reliefs; ancient alluvial terraces; and the actual alluvial plain. Such complexity is echoed in the 60 soil typological units, which were aggregated into 46 soil mapping units, as shown in Fig. 3. The climate is typically Mediterranean, characterized by warm, dry summers and cool, mild winters, with a mean annual rainfall of around 1000 mm, mainly distributed between autumn and winter, and a mean annual temperature of around 15 °C (Alfieri et al., 2019).

4.2. Hydraulic properties dataset

In each representative profile of the soil mapping units, undisturbed soil samples were collected from the horizons using cylindrical steel samplers (8.5 cm diameter and 12.0 cm high). In the laboratory, the samples were saturated by slowly wetting from the bottom in order to remove all the air entrapped in the soil. The maximum water content, θ_0, was gravimetrically determined and the saturated hydraulic conductivity, k_s, was measured by a falling-head permeameter (Reynolds and Elrick, 2002). Then, the Wind method (Arya, 2002), was applied to simultaneously determine the water retention and hydraulic conductivity functions by subjecting the soil samples to an evaporation process. After sealing the bottom surface to prevent drainage, during the evaporation process – at appropriate pre-set time intervals - the weight of the whole sample and the pressure head at three different depths were measured. An iterative procedure was applied for estimating the water retention curve from these measurements. Then, the instantaneous profile method was applied to determine the unsaturated hydraulic conductivity.

$\theta_r, \theta_s, \alpha$ and n parameters in Eq. (4) were derived by fitting the soil water retention data; under the restriction $m = l - l/n, \tau$ and k_0 parameters were derived by fitting the hydraulic conductivity data to Eq. (3). Details of the tests and overall calculation procedures are described in Basile et al. (2012). The parameters obtained in the laboratory were then scaled to better reproduce the field behaviour by following the procedure suggested by Basile et al. (2003a, 2006). Finally, for the few soils having considerable stone content, a correction of θ_s and k_s, to take into account the stoniness, was applied (Coppola et al., 2013b).

5. Results and discussion

This section describes and discusses the results of i) the TFM-ext model sensitivity analysis, ii) the model validation against measured data in large soil columns, iii) the comparison of the results obtained with TFM-ext and Hydrus 1D model and iv) the application to the Valle Telesina case study.

5.1. Sensitivity analysis

First, for each parameter, the appropriate theoretical CDF was derived. Table 3 reports the upper (*A*) and lower (*B*) limits of variation, which were inferred from the dataset, the type of transformation applied, the mean, the standard deviation, the coefficient of variation (*CV*) of the original parameter and the value of the minimum deviation (*D*) between the empirical and the fitted CDFs, according to the Kolomogorov-Smirnoff test.

While θ_r was already normally distributed and, thus, no transformation was applied, for θ_s and α, the best transformation was the Johnson hyperbolic arcsine (*SU*). The Johnson log-ratio transformation (*SB*) was chosen for n and τ and eventually, the lognormal distribution for k_0.

The Monte Carlo procedure allowed to perform the model sensitivity analysis. In Fig. 5, only the results of the uncorrelated case are shown, since the parameters shown a small correlation.

From the barplot of the RI toward the variance, it is possible to infer

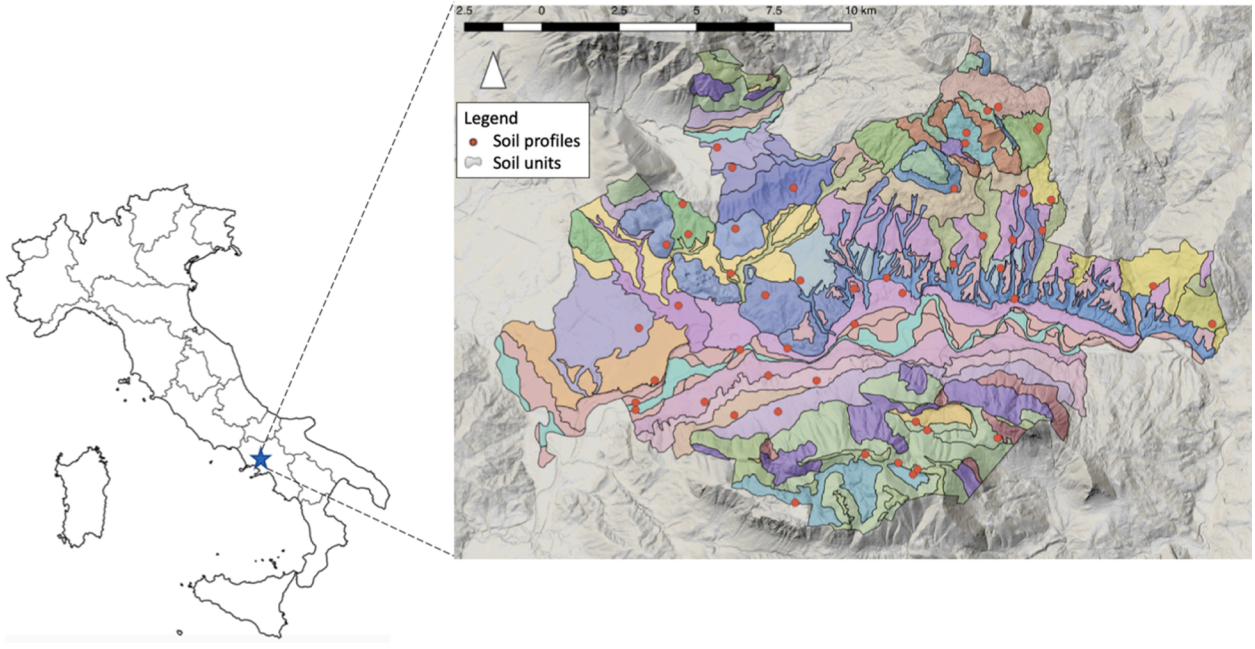

Fig. 3. Localization of the Valle Telesina, Benevento, Italy. The plot on the right shows the soil units (coloured polygons) and the soil sampling points (red dots). (For interpretation of the references to color in this figure legend, the reader is referred to the web version of this article.)

Table 3
Transformation and main statistics of the model parameters: *A* and *B* are the upper and lower bounds of the interval, *NO* stands for no transformation, *SU* stands for the Johnson hyperbolic arcsine and *SB* stands for the Johnson log ratio transformation. The mean, standard deviation and the coefficient of variation (CV) are computed on the measured variables and *D* stands for the Kolomogorov-Smirnoff deviation.

Hydraulic variable	A	B	Transformation	Mean	Standard Deviation	CV	D
θ_r	0.00	0.1	NO	0.002	0.007	2.84	0.21
θ_s	0.20	0.65	SU	0.37	0.121	0.31	0.08
α	0.003	0.1	SU	0.026	0.015	0.58	0.08
n	1.1	3.0	SB	1.29	0.162	0.12	0.19
k_0	1	121	LN	20.76	24.49	1.17	0.12
τ	-8	23	SB	-0.78	4.69	5.97	0.22

some useful information: θ_s and τ are responsible for 32 % and 60 % of the travel times variance, respectively, therefore, the TFM-ext model is mostly sensitive to these parameters. On the contrary, θ_r variability showed no influence at all, while α, n and k_0 showed only a small relative importance (1%, 3%, 4%). The θ_s and τ also show the biggest RD, with 0.25 and 0.50 values, respectively, i.e. the variability in the travel times due to the variation of the two parameters is high, confirming the high sensitivity of the model to those parameters. While the high relative importance of θ_s was somehow expected, since its influence on the flow and transport processes, the high RI of τ and the small RI of k_0 is interesting. τ is usually regarded as an empirical calibration parameter.

The explanation may be found by looking at the impact of these parameters on the shape of the hydraulic conductivity curve in Fig. 1: θ_s and k_s shift the curve along the θ and k axis, respectively, while the parameter τ controls the slope of the curve. For given θ_s and τ, the variation of k_s simply induces a relatively small shift of the curve on the k axis and an elongation of the vertical part of the curve close to saturation. Overall, the change in the k_s may produce significant effects on the travel time pdf only for high top boundary fluxes, thus bringing soil water content close to saturation. In this sense, even a high CV, as observed for the k_s, may only have limited effects on the variability of the travel time pdf. By contrast, the same variation in the water content completely modifies the position of the hydraulic conductivity curve in the $k(\theta)$ plane, with significant effects on the derivative of the $k(\theta)$ and thus on the size of the pores involved in the transport at a given top-boundary flux. In turn, this behavior significantly affects the variability of the travel time pdf. Similar conclusions can be drawn for the parameter τ, with the additional effect of a very high CV, which has itself consequences on the variability of the travel time pdf. This is particularly clear in Fig. 4, where, as an example, the effect of the variability of τ on the hydraulic conductivity curve (left panel) and consequently on the dimensionless flux concentration (i.e., the travel time cdf) (right panel) is shown. Especially in the first part of the curves (e.g., 20 days), clear differences in the values of the travel time cdf can be appreciated between the 4 curves.

The fact that a large CV of an input parameter does not automatically imply large variability in the output has already been discussed in the literature (see, for example, Coppola et al. (2009)). Evidently, the contribution of a parameter to the output depends not so much on its CV as on the sensitivity of the model to the parameter itself.

The sensitivity analysis of the TFM-ext model, with respect to variations in the steady water flux q, was also performed. The parameters were set to their mean values, while q varied between 0.1 and 1 cm d^{-1}. Results of the procedure are reported in Fig. 6, where the blue line represents the evolution of the mean travel times and the red line represents the evolution of the variance of the travel times. Both moments showed the same behaviour: they decreased sharply till a certain q value (around 0.3 cm d^{-1}) and then tended to an asymptotic value of around 45 days and 3000 d^2 for the mean and variance, respectively. Fig. 1 allows to interpret these results as follows: as soon as q increases, more pores contribute to the flow and reduces, indeed, the mean travel times till a certain value. After this value, all the porous space is involved in the flow process till the upper limit of complete saturation ($\theta' = \theta_s$), thus, poorly contributing to both mean and variance TT. In fact, as soon as q increases, even a relatively large variation in its value determines a small variation in θ, till the upper limit θ_s, after which the system produces runoff ($q > k_s$). This is true and holds since the transport in the soil column is considered vertical towards the groundwater. If other mechanisms of runoff generation are considered, such as shallow subsurface flow or surface runoff, then an increase in q would not necessarily decrease the variability in the travel times.

5.2. Soil columns validation

Fig. 7 shows the results of the validation of the TFM-ext for the four soil columns chosen. The dimensionless breakthrough curves, measured (black dots) and simulated (red lines), were compared and some goodness of fit indices were computed. In general, we can observe that the model performs quite well for all the four cases, with the best agreement obtained for the P5 column, where the R^2=0.97, the RMSE = 0.11 and the ME is −0.01 and the less accurate obtained for the P3 column that

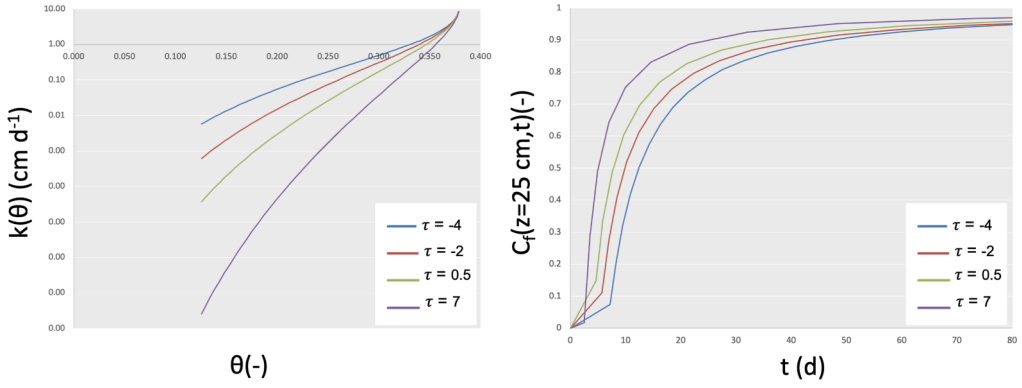

Fig. 4. Variation of the hydraulic conductivity curve (left panel) and of the travel time cdf (right panel) with the parameter τ.

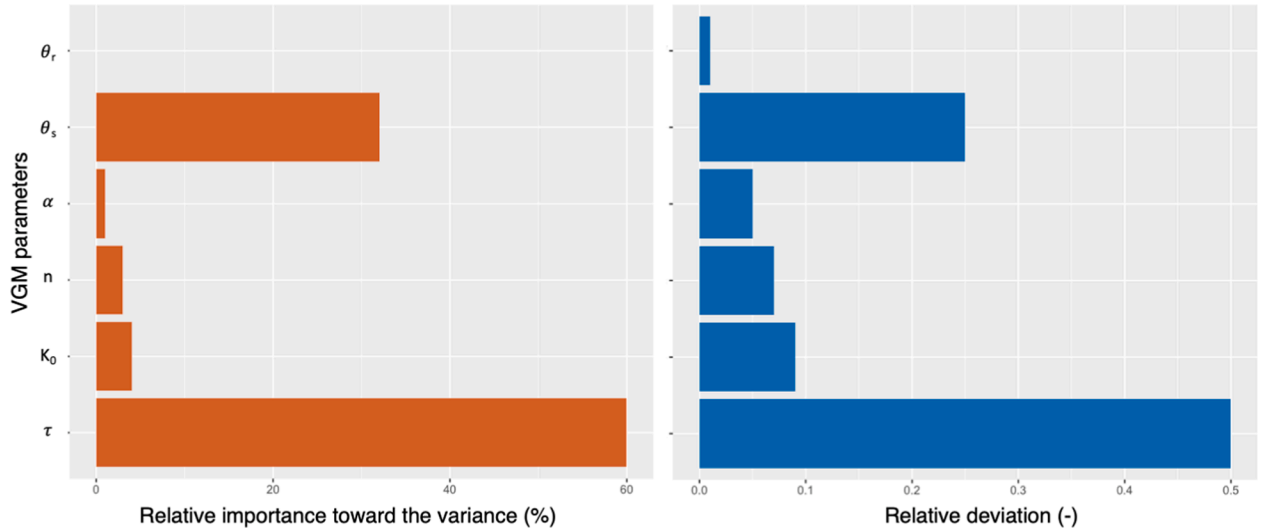

Fig. 5. Relative importance indices toward the variance (red bars) and relative deviation (blue bars). (For interpretation of the references to color in this figure legend, the reader is referred to the web version of this article.)

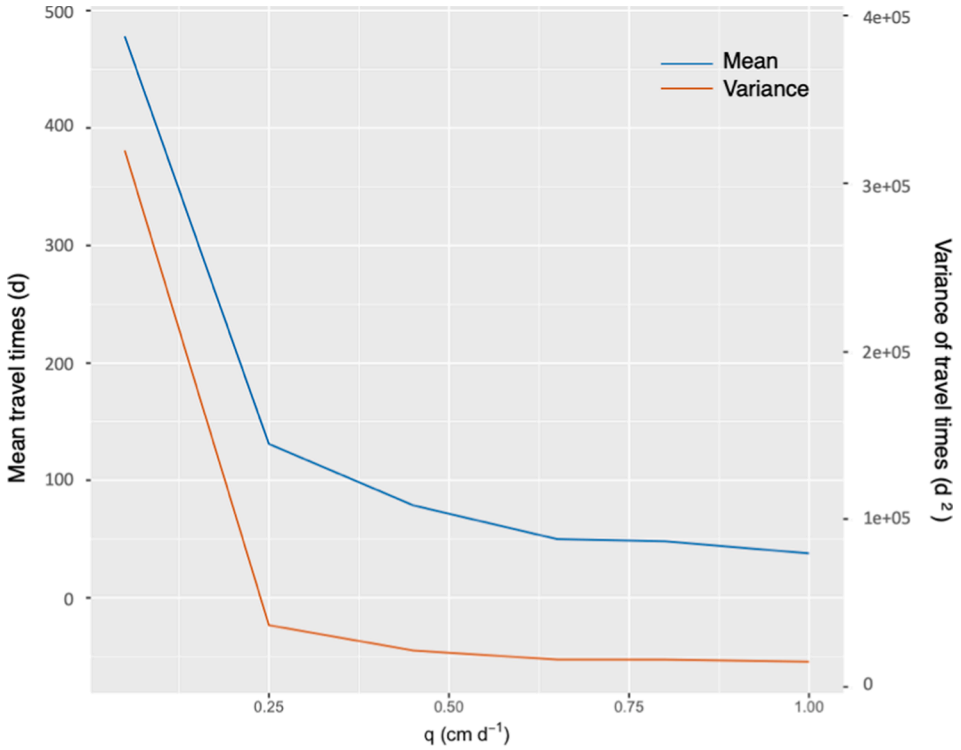

Fig. 6. Model sensitivity analysis with respect to steady flux variations. The blue and the red lines represent the mean and the variance changes with flux, respectively. The y axis reports on the left the value interval of the mean and on the right the value interval of the variance. (For interpretation of the references to color in this figure legend, the reader is referred to the web version of this article.)

still showed a $R^2 = 0.88$, the RMSE = 0.22 and the ME = −0.16, as reported for each graph in the Figure. These results are really promising, since we have to keep in mind that no parameter of the TFM-ext was calibrated.

Overall, we recognize that the three different shapes of breakthrough curves are well reproduced by the TFM-ext model. P1 and P4 columns show a similar behaviour, with an early response and a breakthrough time of around 5 h (0.2 days). P3 column shows an overestimation of solute concentration respect to the measured one, still showing a breakthrough time of around 5 h (0.2 days). P5 column displays a s-shaped breakthrough curve, which is slightly smoother according to the model, with a later breakthrough time of around 12 h (0.45 days).

Despite its important assumptions on the steady state input flux, TFM-ext, through these validation versus real data from large undisturbed soil columns, proved to be robust in reproducing the breakthrough curves for different layered soils, with no calibration of any parameter required. Other validations at field scale in layered soils would not have been feasible at all.

5.3. Hydrus 1D comparison

The moments of the breakthrough curves obtained applying the

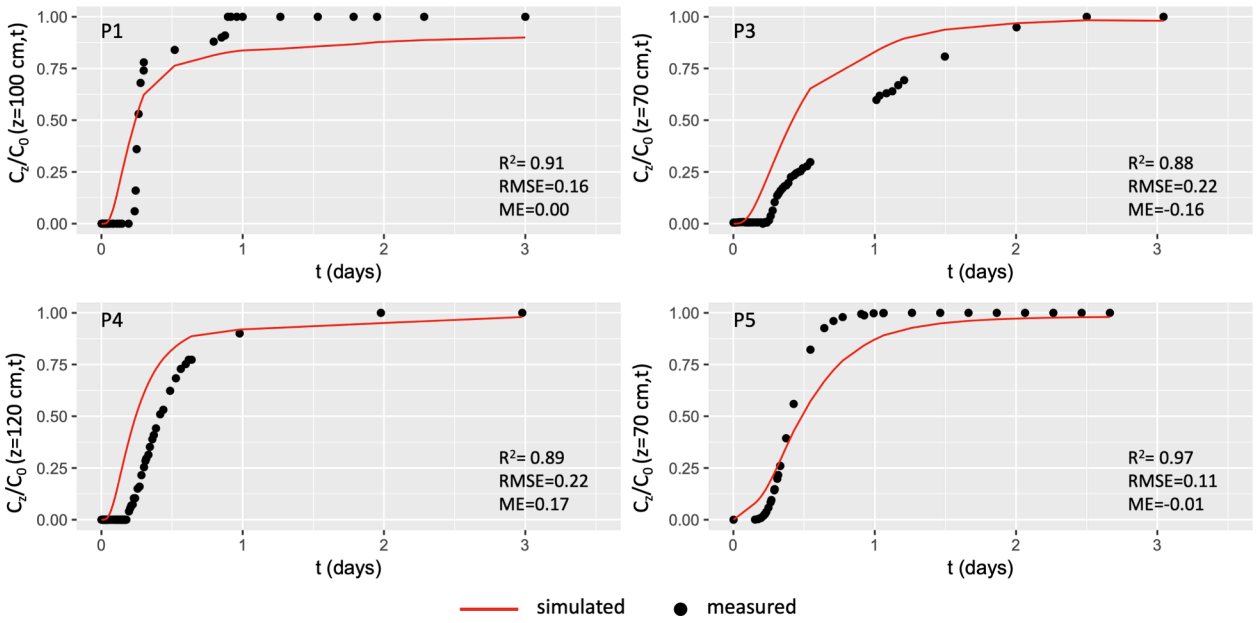

Fig. 7. Validation of the TFM-ext using soil column experiments: red lines represents the simulated dimensionless concentrations while black dots represent measured dimensionless concentrations at the exit depths. (For interpretation of the references to color in this figure legend, the reader is referred to the web version of this article.)

TFM-ext and Hydrus1D at the same soil depth of 150 cm were finally compared for all the soil polygons of the Valle Telesina, as described in Section 3.4.

Results of the application are shown in the scatter plot in Fig. 8, where the black points represent the mean travel times, the black line represents the regression line and the red dashed line represents the bisector. It is immediately clear that there was a really good agreement between the two models, with a correlation coefficient of 0.83, a mean absolute error of around 40 days and a percent bias of −15.8 %. The regression line appears to be almost parallel to the bisector (coefficient of 1.06), with an intercept of 29.3 days. The maximum Hydrus 1D overestimation was obtained for the soil profile ID P32, where the travel times were 199 days using Hydrus 1D and of 109 using the TFM-ext. The higher TT in Hydrus 1D were determined by high k_s values, which, for the lower horizon, was around 430 cm d^{-1}. The variable upper boundary condition determined the soil to be very wet only for short period during rainy events, while remaining rather dry for a longer period, thus leading to a slower response of Hydrus 1D with respect to TFM-ext.

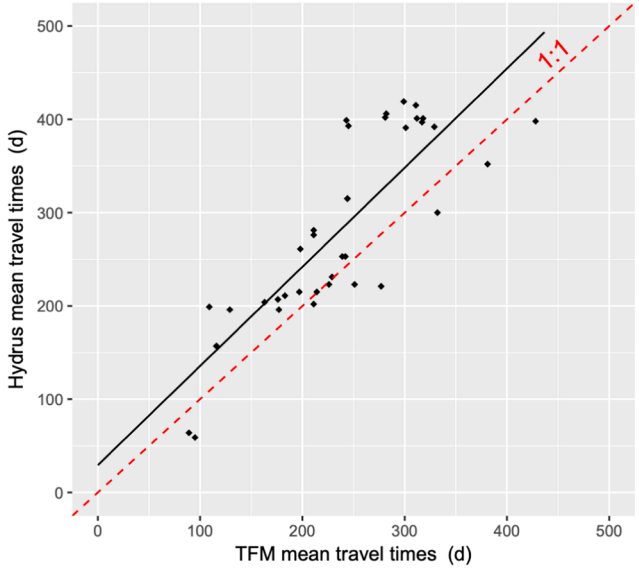

Fig. 8. Scatter plot of the mean travel times obtained using TFM-ext and Hydrus 1D.

Further tests to assess the goodness of the assumption of a log-normal distribution against the use of real data were conducted. We saw that for a greater depth (4 m) and the same flux (0.174 cm/day), a loamy sand showed a mean travel time of 172 days while a clay soil showed a mean travel time of 633 days. Also in these cases we obtained good agreements with Hydrus results, in line with the previous outcomes.

These results are positively surprising and further confirm that the steady state hypothesis underlying the TFM-ext model holds true. Finally, since one of the key points of the proposed model was to be fast, besides being effective, from the computational point of view, the run-time for a single soil profile for Hydrus is between of 3 s and 2 min, while TFM-ext took around 1.2 s to process all the 46 soil profiles.

5.4. *Valle Telesina spatial application*

The spatial application of the TFM-ext to the Valle Telesina case study is shown in Fig. 9. As reported in Section 3, the depth of simulation was 3 m for all the soils. For all profiles, the mean annual precipitation was equal to 795 $mm\ yr^{-1}$ and the reference ET was equal to 950 $mm\ yr^{-1}$. The mean net precipitation varied between 0.112 $cm\ d^{-1}$ and 0.181 $cm\ d^{-1}$ (408 $mm\ yr^{-1}$ and 660 $mm\ yr^{-1}$).

This application is particularly interesting since it allows to compare the different dynamics determined by the multiple soil characteristics and input fluxes, being equals the depth and the land use.

The mean travel times are categorized in ten intervals from 132 (red) to 712 (green) days. It is worth noticing that around the 40% of the soil units, coloured in light green to dark green in the map, have mean travel times above 365 days. These are mainly located on the hills and on the upper part of the mountains (above the 300 m a.s.l.). Given the slow response to the solute injection, these areas shown a good filtering capacity and therefore, could be classified as less vulnerable to possible contaminations compared to the other.

Some soil units present low mean TT, in the interval 132–248 days (red spots on the mountains and the alluvial plain). The red spots on the mountains belong to the same types of soils that, according to the USDA,

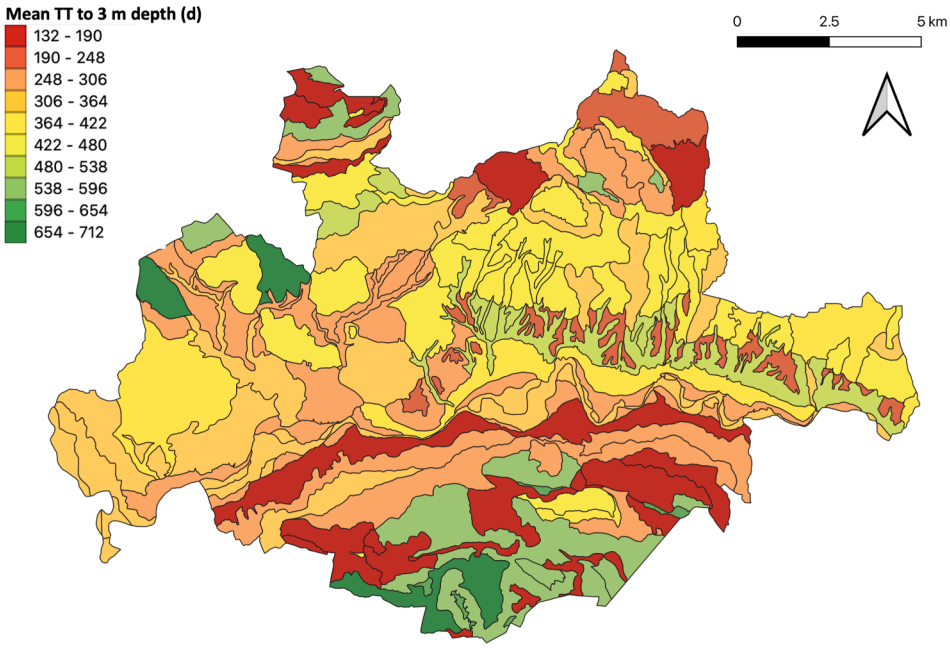

Fig. 9. Map of the mean travel times to 3 m depth associated with the soil units in Valle Telesina. The mean travel times are categorized from the lowest (red colour) to the highest (green color). (For interpretation of the references to color in this figure legend, the reader is referred to the web version of this article.)

are classified as Lithic and Typic Hapludands. This is not surprising because these soils showing andic features, as often mentioned in literature, have distinct hydraulic properties, namely high hydraulic conductivity in wet conditions (similar to sandy soils) and high water retention capacity (similar to clay soils) (Terribile et al., 2018; Bartoli et al., 2007; Basile et al., 2003b). Therefore, since the TFM-ext model is strongly based on the hydraulic conductivity curve and not on the water retention curve, the former prevails and determines the fast TT of soils showing andic features.

The other red spots in the alluvial plain correspond to the soils that are formed on alluvial deposits and classified as Fluvic Cambisols with loamy texture. Because these soils are at the beginning of their pedogenesis, they have a moderately developed soil structure with poor macroporosity and connectivity (Terribile et al., 2011). These pedological features correspond to low values of k_s and high values of τ, thus justifying the lower mean travel times.

6. Conclusion

The purpose of this study was to present the TFM-ext for the estimation of solute travel times to a certain fixed depth, which deploy a simplified statistical approach, based on the transfer functions approach, integrated by soil's physical properties.

In the broad array of leaching models, TFM-ext was conceived to require small computational efforts while being physically-based. In fact, the main reason behind the model was the need to have a fast and effective tool for real-time on-line simulations, required by the new frontier of the web-based Decision Support Systems. The input soil type, the climate, the land use and the crop management are spatially available and real-time overlapped to obtain possible infinite combinations (and model runs) on which to evaluate the NPS travel times.

According to TFM-ext, it is possible to derive the travel times pdf based on the hydraulic conductivity function and characteristic of each layer of the soil. Moreover, the model extends the transport process to the generic depth z, where information on the hydraulic properties couldn't be available, making the assumption of a lognormal travel time pdf, whose parameters are scaled according to the generalized transfer function model.

The sensitivity analysis of the model toward its parameter variations showed that θ_s and τ determine the greatest variability of the travel times, even with relatively small variations.

The validation of the model, performed on four large soil columns, gave very satisfactory results, with a really good agreement between the measured and simulated solute concentrations.

The comparison with the travel times obtained using Hydrus 1D model, which represents our benchmark reference, gave very good results, with high correlation coefficients, small mean absolute errors and small percent bias.

Finally, the application at Valle Telesina extent shown how the model could be used to interpret the different responses of the soils, given a user-defined area, depth, land use and crop management.

In general, for the small computational demand and number of parameters, we can state that TFM-ext met our goals. In this view, the TFM-ext model was integrated as an operative tool for the groundwater vulnerability assessment within the web-based geo-spatial decision support system LandSupport (www.landsupport.eu), which is developed under H2020 project LandSupport. Further improvements of the model will include the reactive transport, in order to be fully operational in support of the pesticides and nitrates directives.

CRediT authorship contribution statement

Marialaura Bancheri: Conceptualization, Methodology, Formal analysis, Software, Data curation, Validation, Writing - original draft. **Antonio Coppola:** Conceptualization, Methodology, Formal analysis, Supervision, Writing - review & editing. **Angelo Basile:** Conceptualization, Methodology, Formal analysis, Data curation, Writing - review & editing, Supervision, Funding acquisition.

Declaration of Competing Interest

The authors declare that they have no known competing financial interests or personal relationships that could have appeared to influence the work reported in this paper.

Acknowledgement

This research was funded by EC H2020 LANDSUPPORT project,

Grant No. 774234.

Appendix A. Time derivative of the hydraulic conductivity function

In the following, all the steps to obtain of the (travel) time derivative of the hydraulic conductivity function are reported. Firstly, the derivative of the hydraulic conductivity function respect to θ is obtained as follows:

$$\frac{dk(\theta)}{d\theta} = \frac{k_0 S_e^{\tau-1}[1-(1-S_e^{1/m})^m][\tau + 2S_e^{1/m}(1-S_e^{1/m})^{m-1} - \tau(1-S_e^{1/m})^m)]}{\theta_s - \theta_r} \tag{A.1}$$

Having defined the flow velocity in the soil (Scotter and Ross, 1994) as:

$$v(\theta) = \frac{dk(\theta)}{d\theta} = \frac{z}{t} \tag{A.2}$$

then, the travel time t is computed as:

$$t = \frac{z}{\frac{dk(\theta)}{d\theta}} = \frac{z}{\frac{k_0 S_e^{\tau-1}[1-(1-S_e^{1/m})^m][\tau+2S_e^{1/m}(1-S_e^{1/m})^{m-1}-\tau(1-S_e^{1/m})^m)]}{\theta_s-\theta_r}} \tag{A.3}$$

Combining Eqs. (3) and (A.3), we obtain the hydraulic conductivity function as a function of the travel time t:

$$k(\theta) = \frac{z[1-(1-S_e^{1/m})^m]}{\frac{tSe^{-1}[\tau+2S_e^{1/m}(1-S_e^{1/m})^{m-1}-\tau(1-S_e^{1/m})^m)]}{\theta_s-\theta_r}} \tag{A.4}$$

Then its travel time derivative is straightforward obtained as:

$$\frac{dk(\theta)}{dt} = -\frac{z[1-(1-S_e^{1/m})^m]}{\frac{t^2Se^{-1}[\tau+2S_e^{1/m}(1-S_e^{1/m})^{m-1}-\tau(1-S_e^{1/m})^m)]}{\theta_s-\theta_r}} \tag{A.5}$$

Appendix B. Supplementary data

Supplementary data associated with this article can be found, in the online version, athttps://doi.org/10.1016/j.jhydrol.2021.126157.

References

Ahuja, L., Rojas, K., Hanson, J., 2000. Root Zone Water Quality Model: Modelling Management Effects on Water Quality and Crop Production. Water Resources Publication.

Alfieri, S., Riccardi, M., Menenti, M., Basile, A., Bonfante, A., De Lorenzi, F., 2019. Adaptability of global olive cultivars to water availability under future mediterranean climate. Mitigation and Adaptation Strategies for Global Change 24, 435–466.

Allen, R.G., Pereira, L.S., Raes, D., Smith, M., et al., 1998. Crop evapotranspiration-guidelines for computing crop water requirements-fao irrigation and drainage paper 56. Fao, Rome 300, D05109.

Aller, L., 1985. DRASTIC: a standardized system for evaluating ground water pollution potential using hydrogeologic settings. Robert S. Kerr Environmental Research Laboratory, Office of Research and Development, US Environmental Protection Agency.

Arya, L., 2002. Wind and hot-air methods. Methods of Soil Analysis: Part 4 Physical Methods, pp. 916–926.

Avanidou, T., Paleologos, E.K., 2002. Infiltration in stratified, heterogeneous soils: Relative importance of parameters and model variations. Water Resources Research 38, 14–1.

Bartoli, F., Regalado, C., Basile, A., Buurman, P., Coppola, A., 2007. Physical properties in european volcanic soils: A synthesis and recent developments. In: Soils of Volcanic Regions in Europe. Springer, pp. 515–537.

Basile, A., Ciollaro, G., Coppola, A., 2003a. Hysteresis in soil water characteristics as a key to interpreting comparisons of laboratory and field measured hydraulic properties. Water Resources Research 39.

Basile, A., Mele, G., Terribile, F., 2003b. Soil hydraulic behaviour of a selected benchmark soil involved in the landslide of sarno 1998. Geoderma 117, 331–346.

Basile, A., Coppola, A., De Mascellis, R., Randazzo, L., 2006. Scaling approach to deduce field unsaturated hydraulic properties and behavior from laboratory measurements on small cores. Vadose Zone Journal 5, 1005–1016.

Basile, A., Buttafuoco, G., Mele, G., Tedeschi, A., 2012. Complementary techniques to assess physical properties of a fine soil irrigated with saline water. Environmental Earth Sciences 66, 1797–1807.

Bongaarts, J., Feeney, G., 2003. Estimating mean lifetime. Proceedings of the National Academy of Sciences 100, 13127–13133.

Botter, G., Bertuzzo, E., Rinaldo, A., 2011. Catchment residence and travel time distributions: The master equation. Geophysical Research Letters 38.

Bouma, J., 2015. Engaging soil science in transdisciplinary research facing - wicked - problems in the information society. Soil Science Society of America Journal 79, 454–458.

Bouma, J., De Vos, J., Sonneveld, M., Heuvelink, G., Stoorvogel, J., 2008. The role of scientists in multiscale land use analysis: lessons learned from dutch communities of practice. Advances in Agronomy 97, 175–237.

Calabrese, S., Porporato, A., 2015. Linking age, survival, and transit time distributions. Water Resources Research 51, 8316–8330.

Carsel, R.F., Parrish, R.S., 1988. Developing joint probability distributions of soil water retention characteristics. Water Resources Research 24, 755–769.

Coppola, A., Santini, A., Botti, P., Vacca, S., Comegna, V., Severino, G., 2004. Methodological approach for evaluating the response of soil hydrological behavior to irrigation with treated municipal wastewater. Journal of Hydrology 292, 114–134.

Coppola, A., Basile, A., Comegna, A., Lamaddalena, N., 2009. Monte carlo analysis of field water flow comparing uni-and bimodal effective hydraulic parameters for structured soil. Journal of Contaminant Hydrology 104, 153–165.

Coppola, A., Comegna, A., Dragonetti, G., Dyck, M., Basile, A., Lamaddalena, N., Kassab, M., Comegna, V., 2011. Solute transport scales in an unsaturated stony soil. Advances in Water Resources 34, 747–759.

Coppola, A., Comegna, A., Dragonetti, G., De Simone, L., Lamaddalena, N., Zdruli, P., Basile, A., 2013a. A stochastic texture-based approach for evaluating solute travel times to groundwater at regional scale by coupling gis and transfer function. Procedia Environmental Sciences 19, 711–722.

Coppola, A., Dragonetti, G., Comegna, A., Lamaddalena, N., Caushi, B., Haikal, M., Basile, A., 2013b. Measuring and modeling water content in stony soils. Soil and Tillage Research 128, 9–22.

Di Guardo, A., Finizio, A., 2015. A client–server software for the identification of groundwater vulnerability to pesticides at regional level. Science of the Total Environment 530, 247–256.

Feddes, R., Kowalik, P., Zaradny, H., 1978. Simulation of field water use and crop yield. simul. monog. pudoc, wageningen, the netherlands. Simulation of field water use and crop yields. Simul. Monogr. Pudoc, Wageningen, the Netherlands.

Fenton, O., Schulte, R.P., Jordan, P., Lalor, S.T., Richards, K.G., 2011. Time lag: a methodology for the estimation of vertical and horizontal travel and flushing timescales to nitrate threshold concentrations in irish aquifers. Environmental Science & Policy 14, 419–431.

Hamby, D., 1995. A comparison of sensitivity analysis techniques. Health Physics 68, 195–204.
Hamlen, C., Kachanoski, R., 1992. Field solute transport across a soil horizon boundary. Soil Science Society of America Journal 56, 1716–1720.
Harman, C.J., 2015. Time-variable transit time distributions and transport: Theory and application to storage-dependent transport of chloride in a watershed. Water Resources Research 51, 1–30.
Holman, I.P., Dubus, I.G., Hollis, J., Brown, C.D., 2004. Using a linked soil model emulator and unsaturated zone leaching model to account for preferential flow when assessing the spatially distributed risk of pesticide leaching to groundwater in england and wales. Science of the Total Environment 318, 73–88.
Johnson, N.L., Kotz, S., Balakrishnan, N., 1970. Continuous Univariate Distributions, vol. 1. Houghton Mifflin Boston.
Jury, W.A., 1982. Simulation of solute transport using a transfer function model. Water Resources Research 18, 363–368.
Jury, W.A., Roth, K., et al., 1990. Transfer Functions and Solute Movement Through Soil: Theory and Applications. Birkhäuser Verlag AG.
Kumar, A., Kanwar, R.S., Singh, P., Ahuja, L.R., 1999. Evaluation of the root zone water quality model for predicting water and no3–n movement in an iowa soil. Soil and Tillage Research 50, 223–236.
Lee, J., Casey, F.X., 2005. Development and evaluation of a simplified mechanistic-stochastic method for field-scale solute transport prediction. Soil Science 170, 225–234.
Leij, F.J., Dane, J., 1991. Solute transport in a two-layer medium investigated with time moments. Soil Science Society of America Journal 55, 1529–1535.
Manna, P., Bonfante, A., Colandrea, M., Di Vaio, C., Langella, G., Marotta, L., Mileti, F.A., Minieri, L., Terribile, F., Vingiani, S., et al., 2020. A geospatial decision support system to assist olive growing at the landscape scale. Computers and Electronics in Agriculture 168, 105143.
Marano, G., Langella, G., Basile, A., Cona, F., De Michele, C., Manna, P., Teobaldelli, M., Saracino, A., Terribile, F., 2019. A geospatial decision support system tool for supporting integrated forest knowledge at the landscape scale. Forests 10, 690.
Paleologos, E.K., Lerche, I., 1999. Multiple decision-making criteria in the transport and burial of hazardous and radioactive wastes. Stochastic Environmental Research and Risk Assessment 13, 381–395.
Petach, M., Wagenet, R., DeGloria, S., 1991. Regional water flow and pesticide leaching using simulations with spatially distributed data. Geoderma 48, 245–269.
Reynolds, W., Elrick, D., 2002. 3.4. 3.3 constant head well permeameter (vadose zone). Methods of Soil Analysis: Part 4 Physical Methods, pp. 844–858.
Rigon, R., Bancheri, M., Formetta, G., de Lavenne, A., 2016a. The geomorphological unit hydrograph from a historical-critical perspective. Earth Surface Processes and Landforms 41, 27–37.
Rigon, R., Bancheri, M., Green, T.R., 2016b. Age-ranked hydrological budgets and a travel time description of catchment hydrology. Hydrology and Earth System Sciences 20, 4929–4947.
Rinaldo, A., Beven, K.J., Bertuzzo, E., Nicotina, L., Davies, J., Fiori, A., Russo, D., Botter, G., 2011. Catchment travel time distributions and water flow in soils. Water Resources Research 47.
Scotter, D., Ross, P., 1994. The upper limit of solute dispersion and soil hydraulic properties. Soil Science Society of America Journal 58, 659–663.
Simunek, J., Sejna, M., Van Genuchten, M.T., Šimnek, J., Šejna, M., Jacques, D., Šimnek, J., Mallants, D., Saito, H., Sakai, M., 1998. Hydrus-1d. Simulating the one-dimensional movement of water, heat, and multiple solutes in variably-saturated media, version 2.
Simunek, J., Van Genuchten, M.T., Šejna, M., 2012. The hydrus software package for simulating the two-and three-dimensional movement of water, heat, and multiple solutes in variably-saturated porous media. Technical manual, version 2, 258.
Simunek, J., Van Genuchten, M.T., Šejna, M., 2016. Recent developments and applications of the hydrus computer software packages. Vadose Zone Journal 15.
Smith, R.E., Diekkrüger, B., 1996. Effective soil water characteristics and ensemble soil water profiles in heterogeneous soils. Water Resources Research 32, 1993–2002.
Sousa, M.R., Jones, J.P., Frind, E.O., Rudolph, D.L., 2013. A simple method to assess unsaturated zone time lag in the travel time from ground surface to receptor. Journal of Contaminant Hydrology 144, 138–151.
Szymkiewicz, A., Gumuła-Kawęcka, A., Potrykus, D., Jaworska-Szulc, B., Pruszkowska-Caceres, M., Gorczewska-Langner, W., 2018. Estimation of conservative contaminant travel time through vadose zone based on transient and steady flow approaches. Water 10, 1417.
Szymkiewicz, A., Savard, J., Jaworska-Szulc, B., 2019. Numerical analysis of recharge rates and contaminant travel time in layered unsaturated soils. Water 11, 545.
Terribile, F., Coppola, A., Langella, G., Martina, M., Basile, A., 2011. Potential and limitations of using soil mapping information to understand landscape hydrology. Hydrology and Earth System Sciences 15, 3895–3933.
Terribile, F., Agrillo, A., Bonfante, A., Buscemi, G., Colandrea, M., D'Antonio, A., De Mascellis, R., De Michele, C., Langella, G., Manna, P., et al., 2015. A web-based spatial decision supporting system for land management and soil conservation. Solid Earth 6, 903.
Terribile, F., Iamarino, M., Langella, G., Manna, P., Mileti, F.A., Vingiani, S., Basile, A., 2018. The hidden ecological resource of andic soils in mountain ecosystems: evidence from italy. Solid Earth 9, 63–74.
Tiktak, A., De Nie, D., Van Der Linden, T., Kruijne, R., 2002. Modelling the leaching and drainage of pesticides in the netherlands: the geopearl model. Agronomie 22, 373–387.
Van Genuchten, M.T., 1980. A closed-form equation for predicting the hydraulic conductivity of unsaturated soils. Soil Science Society of America Journal 44, 892–898.
Vero, S.E., Healy, M.G., Henry, T., Creamer, R.E., Ibrahim, T.G., Richards, K.G., Mellander, P.E., McDonald, N.T., Fenton, O., 2017. A framework for determining unsaturated zone water quality time lags at catchment scale. Agriculture, Ecosystems & Environment 236, 234–242.
Zhang, R., 2000. Generalized transfer function model for solute transport in heterogeneous soils. Soil Science Society of America Journal 64, 1595–1602.
Zhang, R., Hamerlinck, J.D., Gloss, S.P., Munn, L., 1996. Determination of nonpoint-source pollution using gis and numerical models. Journal of Environmental Quality 25, 411–418.